Punjab University Journal of Mathematics
(ISSN 1016-2526)
Vol. 51(12)(2019) pp. 19-36

Phase transition induced by noise in a predator–prey model with herd behavior

Naveed Iqbal
[1]Mathematics Department, Faculty of Science, University of Hail,
Kingdom of Saudi Arabia

Ranchao Wu
School of Mathematical Sciences, Anhui University,
Hefei, Anhui, 230601, P.R. China

Email[1*]: naveediqbal1989@yahoo.com

Received: 25 May, 2019 / Accepted: 03 October, 2019 / Published online: 01 December, 2019

Abstract. In this article, we explore the effect of noise on pattern emergence in a predator–prey model with herd behavior developed because of stochastic partial differential equations (SPDEs). Under specific level of noise, the system is practically observed twice phase transitions. The multi–scaling approach is extended from single to multiple SPDEs. Dynamical analysis of amplitude equation interprets the structural transitions. Then we find the necessary and sufficient constraint which shows the phenomena of transition from a spacial homogenous state to spatial travelling wave. Noise has an undermining impact on the dynamics of a population by the emergence of the Hopf bifurcation. Finally, theoretical results are illustrated via numerical simulations.

AMS (MOS) Subject Classification Codes: 35K51, 35K57, 92C15
Key Words: Travelling waves; Spacial patterns; Spiral turbulence; stochastic partial differential equations.

1. INTRODUCTION

Broadly noticeable phenomena in natural models are spatial non–homogenous dispensation of quantities of species through various spatial scales and this phenomenon is called spatial patterns. The Process behind the emergence of a spatial pattern is one of the main problems in biological science. In 1952, Alan M. Turing exhibit that in a chemical model how the coupling of reaction–diffusion can generate pattern formation [36]. In the past few decades, some experts and scholars have performed a methodical study on different reaction–diffusion model and emergence of patterns, such as the activator–inhibitor system [13, 48, 20, 7], the Brusselator model [11, 3], the FitzHugh–Nagumo model [15, 49], the

Gray–Scott model [18, 42, 17] and so on. Nowadays, the emergence of patterns attains great popularity from researchers that spatial patterns appear in the result of interaction among different biological and physical operations [4, 16, 22, 21, 5, 35, 25, 45, 46].

The impact of noise is a famous area in various fields ranging from physics to biology and chemistry [10]. Recently, it is identified that in theoretical ecology noise is a key tool. Some important queries in population–environment are connected to the part that noise can affect the dynamics of the ecosystem such as weather forcing and non–linear interplay allying individualists of same or distinct species [26]. The impact of noise produced on population dynamics have been studied by [32].

In natural ecosystem the surrounding noise holds an essential role in phase transitions [2, 8, 9, 31, 37, 38, 39]. From the mathematical point of view, in the form of travelling waves the Hopf bifurcation generates a phase transition from spacial homogeneous state to regular fluctuation [27, 40, 41]. When the density of the species in the start is same at equilibrium the traveling wave appears near the spacial defect point. Related to the surrounding the travelling waves have been observed, while the spacial structure of travelling waves is not forever stable. A chemical observation [19] reveals that after the large interval of time the regular spacial waves break into irregular turbulence. As the behavior of the solution does not hold the theory of the reaction–diffusion model near the spacial defect point. The phenomena which produce second phase transition is still unclear such that the regular patterns develop into irregular patterns. To understand the behavior of second phase transition numerical scheme is usually applied.

The main objective of this paper is to consider the travelling waves and investigate the impact of phase transition induced by noise in a predator–prey system with herd behavior. Our study tells us that the emergence of the Hopf bifurcation by noise reveal an undermining effect on the homogeneous state. With regular noise dynamics in the transitional time, regular travelling waves are developed meticulously. The developing regime of travelling waves slowly breaks and is unstable. Irregular turbulence will appear in the end. For long period of time the regular regimes and irregular regimes exist together nevertheless the irregular regimes eventually takes the region from the regular regimes and remains forever.

This article has been arranged as follows: In Section (2) we introduce the mathematical model with the noise term in it. In section (3) the multi–scaling approach is applied to get the necessary and sufficient conditions for noise to generate the Hopf bifurcation from the amplitude equation. In section (4) to verify the theoretical analysis, numerical simulation is applied to obtain the travelling wave.

2. MATHEMATICAL MODEL

In the form of square root of prey population the functional response of prey which reveal herd behavior, the basic predator–prey system with logistic growth is as follow

$$\begin{aligned}\frac{dU}{dt} &= GU\left(1-\frac{U}{C_1}\right)-\frac{E\sqrt{U}V}{1+T_HE\sqrt{U}}\\ \frac{dV}{dt} &= \frac{C_2E\sqrt{U}V}{1+T_HE\sqrt{U}}-DV,\end{aligned} \tag{2.1}$$

where $U(t)$ denotes the density of prey and time t and $V(t)$ denotes the density of predator at time t. The parameter G is the developing rate of the prey. The parameter C_1 represents the capacity of carrying for the prey and in the negligence of prey, the parameter D is the extinction rate of the predator. The parameter E is the searching capability of U for V, C_2 is the consuming rate of prey to predator. The parameter T_H is average time handling.

For understandability, the model (2.1) can be non–dimensionalized by using the following scales:

$$P = \frac{U}{C_1},\ Q = \frac{EV}{G\sqrt{C_1}},\ t_{new} = Gt_{old},$$

where the remaining parameters are dimensionless which are

$$s = \frac{D}{G},\ c = \frac{E\sqrt{C_1}}{G}C_2,\ \alpha = T_H E\sqrt{C_1}.$$

With these scaling model (2.1) becomes

$$\begin{aligned}\frac{dP}{dt} &= P\big(1-P\big) - \frac{\sqrt{P}Q}{1+\alpha\sqrt{P}}\\ \frac{dQ}{dt} &= \frac{c\sqrt{P}Q}{1+\alpha\sqrt{P}} - sQ.\end{aligned} \tag{2.2}$$

On the other hand, the issue of spatial and temporal pattern formation in biological communities is probably one of the most exciting problems in modern biology and ecology. Spatial pattern formation arose from the observation in chemistry by Turing [36] that diffusion can also destabilize equilibrium solution, a scenario well known as Turing instability. Although this is counter intuitive, the interest in the diffusion-driven instability has long expanded from chemical system to biological [23, 1, 12, 29, 30, 44, 28]. Thus by adding the reaction term to the system (2.2) we obtained the reaction–diffusion predator–prey model with herd behavior is as follows

$$\begin{aligned}\frac{\partial P}{\partial t} &= D_1\Delta P + P\big(1-P\big) - \frac{\sqrt{P}Q}{1+\alpha\sqrt{P}}\\ \frac{\partial Q}{\partial t} &= D_2\Delta Q + \frac{c\sqrt{P}Q}{1+\alpha\sqrt{P}} - sQ,\end{aligned} \tag{2.3}$$

where the non–negative constants D_1 and D_2 for the prey and predator are diffusion coefficients. Nevertheless, from [47], we know that the phenomenon of spatial pattern formation in (2.3) cannot occur under all possible diffusion rates. So, the researchers in [47, 44] change the linear mortality sQ into the quadratic mortality sQ^2 in (2.3) and investigated Turing Pattern, Stability, Turing instability and Hopf bifurcations.

Let $c = r$, $D_1 = D_2 = 1$, $b = s/r$. We modify the system (2.3) with noise by considering the key role of the noise in population dynamics as follows

$$\begin{aligned}\frac{\partial P}{\partial t} &= \Delta P + P\big(1-P\big) - \frac{\sqrt{P}Q}{1+\alpha\sqrt{P}} + \varphi\eta(t)\\ \frac{\partial Q}{\partial t} &= \Delta Q + \frac{r\sqrt{P}Q}{1+\alpha\sqrt{P}} - rbQ + \varphi\eta(t).\end{aligned}$$

When the diffusion and noise is absent, by basic computation shows that this model has three spatial uniform equilibria such as:
$(0,0)$, $(1,0)$ and $(P_*, Q_*) = \left(\frac{b^2}{(1-\alpha b)^2}, \frac{b\left((1-\alpha b)^2 - b^2\right)}{(1-\alpha b)^4} \right)$.

In [6], when $\alpha = 0$ the average time handling is zero, the author has used this supposition. Following the work of [6] throughout in this paper, we also assume that $\alpha = 0$ which implies

$$\begin{aligned} \frac{\partial P}{\partial t} &= \Delta P + P\big(1-P\big) - \sqrt{P}Q + \varphi\eta(t) \\ \frac{\partial Q}{\partial t} &= \Delta Q + rQ\big(\sqrt{P} - b\big) + \varphi\eta(t), \end{aligned} \tag{2.4}$$

where φ is the noise tensor, $\eta(t)$ is the arbitrary Gaussian variation which holds $\langle \eta(t) \rangle = 0$ and $\langle \eta(t)\eta(\tau) \rangle = 2\varphi(t-\tau)$, i.e. the Gaussian variation $\eta(t)$ is different in time and consistent in space. We examined the system (2.4) under zero flux boundary constraints, biologically we can say that there is no flux over the boundary of the population.

3. PHASE TRANSITION INDUCED BY NOISE

We call the system (2.4) a deterministic system in the absence of noise. When the diffusion is absent, basic computation shows that the model (2.4) has three spacial uniform equilibria which consists of two boundary equilibriums $(0,0)$, $(1,0)$ and a positive equilibrium $(P_0, Q_0) = (b^2, b(1-b^2)$ where $b \in (0,1)$. The Jacobian matrix J is as follows

$$J = \begin{pmatrix} \frac{1-3b^2}{2} & -b \\ \frac{r(1-b^2)}{2} & 0 \end{pmatrix} = \begin{pmatrix} J_{11} & J_{12} \\ J_{21} & J_{22} \end{pmatrix}.$$

From the biological point of view, we only focused the behavior of stability of positive equilibrium point. In this case the positive spacial uniform equilibrium if $b > \sqrt{\frac{1}{3}}$ it is a stable node. If $b < \sqrt{\frac{1}{3}}$ it is near to a stable limit cycle. Thus the system (2.4) undergoes the critical value of the Hopf bifurcation parameter b:

$$b = \sqrt{\frac{1}{3}} \equiv b_H.$$

When $b > b_H$, we shall show that noise undermines the stable node to produce the alternate dynamics. Multi–scaling analysis will apply near the Hopf bifurcation point. For the solution of system (2.4) the Fourier expansion is as follows

$$\begin{pmatrix} P \\ Q \end{pmatrix} = \begin{pmatrix} P_0 \\ Q_0 \end{pmatrix} + \sum_k \exp(\lambda(k)t). \tag{3.5}$$

Near the Hopf bifurcation value b_H, the amplitude $\lambda(k_H) \approx 0$ correspond the wave–number $k_H = 0$. All the amplitudes $\lambda(k \neq k_H) \ll 0$, expect for $k_H = 0$. The amplitude $\lambda(k_H)$ dominate the other amplitudes by using central manifold theorem. Based on the stability of the spatial uniform solution, we consider a perturbation as follows

$$\tilde{P}(t) = P(t) - P_0,\ \tilde{Q}(t) = Q(t) - Q_0.$$

For the sake of convenience, we omit tildes. At the positive equilibrium (P_0, Q_0), by utilizing the expansion system (2.4) can obtain as

$$\begin{aligned}
\frac{\partial P}{\partial t} &= \Delta p + J_{11}P + J_{12}Q + \frac{1-9b^2}{8b^2}P^2 - \frac{1}{2b}PQ - \frac{1-b^2}{16b^4}P^3 \\
&+ \frac{1}{8b^3}P^2Q + \mathcal{O}(\rho^3) + \varphi\eta(t) \\
\frac{\partial Q}{\partial t} &= \Delta Q + J_{21}P + J_{22}Q - \frac{\gamma(1-b^2)}{8b^2}P^2 + \frac{r}{2b}PQ + \frac{r(1-b^2)}{16b^4}P^3 \\
&- \frac{r}{8b^3}P^2Q + \mathcal{O}(\rho^3) + \varphi\eta(t),
\end{aligned} \tag{3.6}$$

For multi–scaling analysis, we let $t = \omega T + \epsilon\tau_1 + \epsilon^2\tau_2 + \mathcal{O}(\epsilon^3)$ where the variable t depends on $T,\ \tau_1,\ \tau_2$ and ϵ is infinitesimal. T is the fast time scale with same order as t, where τ_1 and τ_2 are slow time scale and of high order as t. We let $\epsilon^2 = \frac{b-b_H}{b_H}$, and the term noise φ is small related to ϵ^2. The dynamics has a fast time scale close to the value of Hopf bifurcation, $t \sim 2\pi/\omega$ where $\omega = \sqrt{\frac{rb(1-b)}{2}}$ is the fast mode frequency. We set the multi–scaling analysis as follows

$$\begin{aligned}
\begin{pmatrix} P \\ Q \end{pmatrix} &= \epsilon \begin{pmatrix} P_1 \\ Q_1 \end{pmatrix} + \epsilon^2 \begin{pmatrix} P_2 \\ Q_2 \end{pmatrix} + \epsilon^3 \begin{pmatrix} P_3 \\ Q_3 \end{pmatrix} + \mathcal{O}(\epsilon^4), \\
\frac{\partial}{\partial t} &= \omega\frac{\partial}{\partial T} + \frac{\partial}{\partial \tau_1}\epsilon + \frac{\partial}{\partial \tau_2}\epsilon^2 + \mathcal{O}(\epsilon^3), \\
b - b_H &= b_H\epsilon^2 + \mathcal{O}(\epsilon^3), \\
\varphi &= \varphi_0\epsilon^3 + \mathcal{O}(\epsilon^4),
\end{aligned} \tag{3.7}$$

where P_i and Q_i $(i = 1, 2, 3)$ are slow time scale solution behavior.

Substituting (3.7) into the system (3.6) and comparing the same power of ϵ, one can obtain the three equations as follows:

$$\begin{aligned}
\mathcal{O}(\epsilon) : \left(\omega\frac{\partial}{\partial T}\mathbf{I} - \mathbf{L_H}\right) \begin{pmatrix} P_1 \\ Q_1 \end{pmatrix} &= 0, \\
\mathcal{O}(\epsilon^2) : \left(\omega\frac{\partial}{\partial T}\mathbf{I} - \mathbf{L_H}\right) \begin{pmatrix} P_2 \\ Q_2 \end{pmatrix} &= \mathbf{B}, \\
\mathcal{O}(\epsilon^3) : \left(\omega\frac{\partial}{\partial T}\mathbf{I} - \mathbf{L_H}\right) \begin{pmatrix} P_3 \\ Q_3 \end{pmatrix} &= \mathbf{C}.
\end{aligned} \tag{3.8}$$

Here

$$\begin{aligned}
\mathbf{L_H} &= \begin{pmatrix} 0 & -\sqrt{\frac{1}{3}} \\ \frac{r}{3} & 0 \end{pmatrix}, \\
\mathbf{B} &= \begin{pmatrix} \frac{1-9b^2}{8b^2}P_1^2 - \frac{1}{2b}P_1Q_1 \\ -\frac{r(1-b^2)}{8b^2}P_1^2 + \frac{r}{2b}P_1Q_1 \end{pmatrix}, \\
\mathbf{C} &= b_H \begin{pmatrix} -\sqrt{3} & -1 \\ -\frac{r}{\sqrt{3}} & 0 \end{pmatrix}\begin{pmatrix} P_1 \\ Q_1 \end{pmatrix} - \frac{\partial}{\partial \tau_2}\begin{pmatrix} P_1 \\ Q_1 \end{pmatrix} \\
&+ \begin{pmatrix} \frac{1-9b^2}{4b^2}P_1Q_2 - \frac{1}{2b}\Big(P_1Q_2 + P_2Q_1\Big) - \frac{1-b^2}{16b^4}P_1^3 + \frac{1}{8b^3}P_1^2Q_1 \\ -\frac{r(1-b^2)}{4b^2}P_1Q_2 + \frac{r}{2b}\Big(P_1Q_2 + P_2Q_1\Big) + \frac{r(1-b^2)}{16b^4}P_1^3 - \frac{r}{8b^3}P_1^2Q_1 \end{pmatrix} \\
&+ \begin{pmatrix} \varphi_0 \\ \varphi_0 \end{pmatrix}\eta(t). \qquad (3.9)
\end{aligned}$$

Since $\mathbf{L_H}$ linear operator of the system and $(P_1, Q_1)^T$ is the linear combination of the eigenvector related to the eigenvalue $i\omega$. We first consider the case $\mathcal{O}(\epsilon)$ and the solution is given by

$$(P_1, Q_1)^T = \varrho C(\tau_1, \tau_2)e^{iT} + c.c., \text{ with } \varrho \equiv (\varrho_1, \varrho_2)^T \in Ker(\mathbf{L_H} - i\omega\mathbf{I}), \qquad (3.10)$$

where $C(\tau_1, \tau_2)$ is the arbitrary amplitude of the solution and $c.c.$ stands for the complex conjugate. Its form is intended by higher order perturbational term. The vector ϱ is defined up to a constant and normalized as follows

$$\varrho = (1, \varrho_2)^T, \text{ with } \varrho_2 = -i\sqrt{\frac{r(\sqrt{3}-1)}{2}}. \qquad (3.11)$$

Next, we consider the case of $\mathcal{O}(\epsilon^2)$. Substituting (3.10) into system (3.8), we obtain

$$\mathbf{B} = \begin{pmatrix} \frac{1-9b^2}{8b^2}\big(|C\varrho_1|^2 + C^2\varrho_1^2 e^{2iT}\big) - \frac{1}{4b}|C|^2\big(\varrho_1\bar{\varrho}_2 + \bar{\varrho}_1\varrho_2\big) - \frac{1}{2b}C^2\varrho_1\varrho_2 e^{2iT} \\ -\frac{r(1-b^2)}{8b^2}\big(|C\varrho_1|^2 + C^2\varrho_1^2 e^{2iT}\big) + \frac{r}{4b}|C|^2\big(\varrho_1\bar{\varrho}_2 + \bar{\varrho}_1\varrho_2\big) + \frac{r}{2b}C^2\varrho_1\varrho_2 e^{2iT} \end{pmatrix} + c.c.$$

The right side of the above equation have no resonance (i.e. $\mathbf{B}$ have no term of e^{iT}), by default the Fredholm alternative is hold. We explicitly calculate the solution $\mathbf{B}$ in (3.8)as

$$\begin{pmatrix} P_2 \\ Q_2 \end{pmatrix} = \mid C \mid^2 \begin{pmatrix} f_0 \\ g_0 \end{pmatrix} + C^2 \begin{pmatrix} f_2 \\ g_2 \end{pmatrix} e^{2iT} + c.c.,$$

where $(f_0, g_0)^T$ and $(f_2, g_2)^T$ are the solution of

$$-\mathbf{L_H}\begin{pmatrix} f_0 \\ g_0 \end{pmatrix} = \begin{pmatrix} \frac{1-9b^2}{8b^2}|\varrho_1|^2 - \frac{1}{4b}\big(\varrho_1\bar{\varrho}_2 + \bar{\varrho}_1\varrho_2\big) \\ -\frac{r(1-b^2)}{8b^2}|\varrho_1|^2 + \frac{r}{4b}\big(\varrho_1\bar{\varrho}_2 + \bar{\varrho}_1\varrho_2\big) \end{pmatrix}, \qquad (3.12)$$

$$\big(-\mathbf{L_H} + 2i\mathbf{I}\big)\begin{pmatrix} f_2 \\ g_2 \end{pmatrix} = \begin{pmatrix} \frac{1-9b^2}{8b^2}\varrho_1^2 - \frac{1}{2b}\varrho_1\varrho_2 \\ -\frac{r(1-b^2)}{8b^2}\varrho_1^2 + \frac{r}{2b}\varrho_1\varrho_2 \end{pmatrix}. \qquad (3.13)$$

We now consider $\mathcal{O}(\epsilon^3)$. Assure the existence of the non–trivial solution of this system by using Fredholm alternative condition, where $(\omega\frac{\partial}{\partial T}\mathbf{I} - \mathbf{L_H})^*$ and $(\omega\frac{\partial}{\partial T}\mathbf{I} - \mathbf{L_H})$ are

the adjoint operator of each other. The right hand side of the vector function orthogonal with the non–trivial kernel of $(\omega\frac{\partial}{\partial T}\mathbf{I}-\mathbf{L_H})^*$. The non–trivial kernel of $(\omega\frac{\partial}{\partial T}\mathbf{I}-\mathbf{L_H})^*$ is represented as $\varrho^* e^{iT}$ and

$$\varrho^* e^{iT} \equiv \begin{pmatrix} \varrho_1^* \\ \varrho_2^* \end{pmatrix} e^{iT} = \begin{pmatrix} 1 \\ i\sqrt{\frac{2}{r(\sqrt{3}-1)}} \end{pmatrix} e^{iT}. \tag{3.14}$$

To examine the resonance of the $\mathbf{C}$, the Fredholm alternative condition satisfies $\langle \varrho^* e^{iT}, \mathbf{C}\rangle = 0$, where

$$\langle x(T), y(T)\rangle = \int_0^{2\pi} x^*(T)y(T)dT.$$

One can obtain

$$\begin{aligned} & b_H C(\varrho_1^*, -\varrho_2^*)\begin{pmatrix} -\sqrt{3} & -1 \\ -\frac{r}{\sqrt{3}} & 0 \end{pmatrix}\begin{pmatrix} \varrho_1 \\ \varrho_2 \end{pmatrix} - (\varrho_1^*, -\varrho_2^*)\begin{pmatrix} \varrho_1 \\ \varrho_2 \end{pmatrix}\frac{\partial C}{\partial \tau_2} \\ + \quad & \mid C \mid^2 C(\varrho_1^*, -\varrho_2^*)\begin{pmatrix} \frac{1-9b^2}{4b^2}\big(2f_0\varrho_1 + f_2\bar{\varrho_1}\big) - \frac{1}{2b}\big(2f_0\varrho_2 + f_2\bar{\varrho_2} \\ +2g_0\varrho_1 + g_2\bar{\varrho_1}\big) - \frac{1-b^2}{16b^4}\varrho_1^3 + \frac{1}{8b^3}\varrho_1^2\varrho_2 \\ \\ -\frac{r(1-b^2)}{8b^2}\big(2f_0\varrho_1 + f_2\bar{\varrho_1}\big) + \frac{r}{2b}\big(2f_0\varrho_2 + f_2\bar{\varrho_2} \\ +2g_0\varrho_1 + g_2\bar{\varrho_1}\big) + \frac{r(1-b^2)}{16b^4}\varrho_1^3 - \frac{r}{8b^3}\varrho_1^2\varrho_2 \end{pmatrix} \\ + \quad & \varphi_0(\varrho_1^*, -\varrho_2^*)\begin{pmatrix} 1 \\ 1 \end{pmatrix}\int_0^{2\pi}\eta(T/\omega)e^{-iT}dT = 0. \end{aligned} \tag{3.15}$$

Let the amplitude $A = \epsilon C$ and multiplying (3.15) by ϵ^3, we obtain the amplitude equation

$$\frac{dA}{dt} = (\beta - \beta_H)f_1 A - f_3 A|A|^2 + \varphi(\varrho_1^*, -\varrho_2^*)\omega\int_0^{2\pi/\omega}\eta(t)e^{-i\omega t}dt, \tag{3.16}$$

where

$$\begin{aligned} f_1 &= \varrho_1\Big(-\sqrt{3}\varrho_1^* + \frac{\gamma}{\sqrt{3}}\varrho_2^*\Big) - \varrho_1^*\varrho_2, \\ f_3 &= -(\varrho_1^*, -\varrho_2^*)\begin{pmatrix} \frac{1-9b^2}{4b^2}\big(2f_0\varrho_1 + f_2\bar{\varrho_1}\big) - \frac{1}{2b}\big(2f_0\varrho_2 + f_2\bar{\varrho_2} \\ +2g_0\varrho_1 + g_2\bar{\varrho_1}\big) - \frac{1-b^2}{16b^4}\varrho_1^3 + \frac{1}{8b^3}\varrho_1^2\varrho_2 \\ \\ -\frac{r(1-b^2)}{8b^2}\big(2f_0\varrho_1 + f_2\bar{\varrho_1}\big) + \frac{r}{2b}\big(2f_0\varrho_2 + f_2\bar{\varrho_2} \\ +2g_0\varrho_1 + g_2\bar{\varrho_1}\big) + \frac{r(1-b^2)}{16b^4}\varrho_1^3 - \frac{r}{8b^3}\varrho_1^2\varrho_2 \end{pmatrix}. \end{aligned}$$

We notice that the amplitude $A(t)$ depends on the strength of the noise φ. Furthermore, $Re(f_1) = -\sqrt{3} < 0$, when $\varphi = 0$ the amplitude decompose to 0 if $b > b_H$, which means positive equilibrium (u_0, v_0) is stable in the deterministic system. With the presence of

noise, substituting $\varrho_1^* = 1$ and $\varrho_2^* = i\sqrt{\frac{2}{r(\sqrt{3}-1)}}$ into (3.16) one can obtain,

$$\begin{aligned}\frac{dRe(A)}{dt} &= (b-b_H)(-\sqrt{3})Re(A) + \phi Re(A)^3 + \varphi\omega \int_0^{2\pi/\omega} \eta(t)\Big(\cos(\omega t) \\ &+ \sqrt{\frac{2}{r(\sqrt{3}-1)}}\sin(\omega t)\Big)dt, \end{aligned} \tag{3.17}$$

where the real part of A is $Re(A)$ and ϕ dependent on r. When the phase transition appears, $\phi Re(A)^3$ is terminate by $(b-b_H)(-\sqrt{3})Re(A)$. Thus, after large interval of time the amplitude $A(t)$ tends to positive steady state, if and only if

$$\int_0^{2\pi/\omega} \eta(t)\Big(\cos(\omega t) + \sqrt{\frac{2}{r(\sqrt{3}-1)}}\sin(\omega t)\Big)dt > 0. \tag{3.18}$$

Since the phase transition rely on the noise, we deduce that phase transition produced by noise and undermine the homogeneous state of the system. Hutt [14] Studied that the noise driven the Hopf bifurcation.

Through numerical simulations, we will show that the noise induced phase transitions. Figure. 1 shows that the prey species density found at defined space point. We observe that in the stability of the system (2.4) noise played an essential role. The exact and amplitude solution (obtained from (3.16)) are decomposed to the positive equilibrium point (P_0, Q_0) in the deterministic system (up panel). The exact solution with noise showed alternate behavior (down panel), where amplitude solution holds (3.16).

4. Emergence of travelling wave and breakup

The reaction–diffusion model emerge travelling waves in 2–dimensional space in case of phase transition produced by Hopf bifurcation [33, 34]. Self–composed travelling wave is generated at the core of the spatial defect point. Numerically it will be shown that travelling waves are generated by noise driven phase transition. The simulation shows that travelling waves break into spatial–temporal chaos slowly known as spiral turbulence. In a chemical model, the spiral turbulence was initially determined by [19].

Our numerical scheme depends on the formulae based on stochastic Euler forward finite difference algorithm [43, 48]. Although the section, the system is observe in defined spatial domain $[0, 900] \times [0, 300]$. On a framework the system is determined by step time $\Delta t = 0.1$ and step space $\Delta u = \Delta v = 1$. Numerical scheme of the system is initialized by spatial homogenous population densities distribution for the reason that homogeneity will last till the end by spatial homogenous initial distribution, which is not of our concern. We count the given below initial conditions for comprehensive results.

$$\begin{aligned} P(u,v,0) &= P_0 - \varepsilon_1(u-180)(u-720) - \varepsilon_2(v-90)(v-210), \\ Q(u,v,0) &= Q_0 - \varepsilon_3(u-445) - \varepsilon_4(u-135), \end{aligned} \tag{4.19}$$

where $\varepsilon_1 = 8 \cdot 10^{-7}, \varepsilon_2 = 6 \cdot 10^{-7}, \varepsilon_3 = 9 \cdot 10^{-5}$ and $\varepsilon_4 = 6 \cdot 10^{-5}$.

$$\begin{aligned} P(u,v,0) &= P_0 - \varepsilon_1(u-0.1v-225)(u-0.1v-675), \\ Q(u,v,0) &= Q_0 - \varepsilon_2(u-225) - \varepsilon_3(v-675), \end{aligned} \tag{4.20}$$

where $\varepsilon_1 = 8 \cdot 10^{-7}, \varepsilon_2 = 6 \cdot 10^{-7}, \varepsilon_3 = 9 \cdot 10^{-5}$.

Finding for the prey species is presented in our numerical scheme. Figure. 2 and 4 indicates the systematic emergence of an irregular spatial regime as rising of regular spatial travelling waves as indicated by initial constraints (4.19) and (4.20), while the travelling waves in the initial stage are more regular in Figure. 2(a) than Figure. 4(a). It is shown in (Figure. 2(d) and 4(d)) that the break up in travelling waves begins with the emergence of an irregular spatial regime and in the end, the irregular regime appears in the complete region. The noise played a main part in establishing travelling waves as shown in Figure. 2 and 4 and is not compulsory to demolish the stability of travelling wave. Similarly for the system (2.4), finding for the prey species is presented when average handling time $\alpha \neq 0$. A systematic emergence of an irregular spatial regime as rising of regular spatial travelling waves as shown in Figure. 3 and 5 connected by initial constraints (4.19) and (4.20), while in the initial stage the travelling waves are less regular than in Figure. 3(a) than Figure. 5(a). It is shown in (Figure. 3(d) and 5(d)) that the break up in travelling waves begins with the emergence of an irregular spatial regime and in the end, the irregular regime appears in the complete region. The noise played a main part in establishing travelling waves as shown in Figure. 3 and 5 and is not compulsory to demolish the stability of travelling wave. The cause of break up in travelling waves is not clear.

The emergence and break in the pattern of the system dynamics can be seen in detail in Figure. 6 and Fig. 7. The 2-dimensional energy spectra are indicated by Figure. 6 is a suitable sign of spatial chaotic dynamics [24]. The dynamics of spatial regime show widen character after the large interval of time. The moving path attains at a defined point $(u, v) = (450, 150)$ in the phase region is shown in Figure. 7. We can easily find out that inside the limit cycle the path nearly fills the complete domain. Thus, to divide the domain into two sections a visible boundary at each moment is present such as a regular and irregular regime (jagged pattern) [24]. In addition, the steady expansion in the limit cycle amplitude exhibits increase in the boundary. The irregular regime at the end disperses on the complete domain, which indicates that for a specific large time interval the two dynamical patterns can coincide. We can observe by Figure. 2 and 4 that noise can cause an appearance of chaotic spatial–temporal regime at large time interval which appears to remain forever, while the regular pattern appears at an intermediate time. Figure. 3 and 5 also showed the same observation as mentioned above.

5. Conclusion

In this study the impact of noise on spatial regime dynamics in a predator–prey system with herd behavior is observed. We focused that the model without noise is locally stable under parametric constraint. Sufficient and necessary constraint is constructed for noise by multi-scale analysis to generate the existence of Hopf bifurcation by amplitude equation, which resulted in the appearance of travelling waves evolved into the spatial–temporal chaos.

Before the appearance of spatial–temporal chaos two transitions exist. The Appearance of travelling waves originally by spatial heterogenous population density dispersion is the result of the first transition. The break in travelling waves in spatial–temporal chaos is resulted by the second transition. The mathematical point of view for second transition is ambiguous, while on the other hand multi–scale analysis completely understood. With

noise, this method helps to compute directly the centre manifold and examine its impact on Turing bifurcations. We obtain the bifurcation constrain (3.18) by deriving amplitude equation (3.16). The level of the noise strength φ is not included in bifurcation constrain. On the other hand φ is an order of ϵ^3 such as $\varphi \sim ((b-b_H)/b_H)^{3/2}$ as assumed from (3.7). We find out that the noise can induce the spiral turbulence by a second phase transition.

ACKNOWLEDGMENTS

This work was supported by the National Science Foundation of China (No. 11571016, 61403115, 11971032).

REFERENCES

[1] S. Aly, I. Kim, D. Sheen, *Turing instability for a ratio–dependent predator–prey model with diffusion*, Appl. Math. Comput. **217,** (2011) 7265–7281.

[2] G. Agez, M.G. Clerc, E. Louvergneaux, R.G. Rojas, *Bifurcations of emerging patterns in the presence of additive noise*, Phys. Rev. E, **87,** (2013) 042919–042929.

[3] R. Anguelov, S. M. Stoltz, *Stationary and oscillatory patterns in a coupled Brusselator model*, Math. and Comp. in Sim., **133,** (2017) 39–46.

[4] Y. Astrov, E. Ammelt, S. Teperick, H. G. Purwins, *Hexagon and stripe Turing structures in a gas discharge system*, Phys. Lett. A, **211,** (1996) 184–190.

[5] R.E. Baker, E.A. Gaffney, P.K. Maini, *Partial differential equations for self–organisation in cellular and developmental biology*, Nonlinearity, **21,** (2008) R251–R290.

[6] P. A. Braza, *Predator–prey dynamcis with square root functional responces*, Nonlinear Anal. RWA, 13, (2012) 1837–1843.

[7] M. Banerjee, S. Petrovskii, *Self–organised spatial patterns and chaos in a ratio–dependent predator-prey system*, Theor. Ecol., **4,** (2011) 37–53.

[8] M.G. Clerc, C. Falcón, E. Tirapegui, *Front propagation sustained by additive noise*, Phys. Rev. E, **74,** (2006) 011303–011318.

[9] G. Denaro, D. Valenti, A.L. Cognata, B. Spagnolo, A. Bonanno, G. Basilone, S. Mazzola, S.W. Zgozi, S. Aronica, C. Brunet, *Spatio–temporal behaviour of the deep chlorophyll maximum in mediterranean sea*: Development of a stochastic model for picophytoplankton dynamics, Ecol. Complex., **13,** (2013) 21–34.

[10] J. A. Freund, T. Pöschel (Eds.), *Stochastic Processes in Physics, Chemistry and Biology*, Lecture Notes in Physics, Springer, Berlin, **557,** (2000).

[11] A. A. Golovin, B. J. Matkowsky, V. A. Volpert, *Turing pattern formation in the Brusselator model with superdiffusion*, SIAM J. Appl. Math. **69,**(2008), 251–272.

[12] L. N. Guin, P.K. Mandal, *Spatial pattern in a diffusive predator–prey model with sigmoid ratio-dependent functional response*, Int. J. Biomath. **7 ,**(2014) 1–26. 1450047.

[13] B. I. Henty, T. A. M. Langlands, S. L. *Wearne, Turing pattern formationn in fractional actiator–inhibitor system*, Phys. Rev. E., **72,** (2005) 026101.

[14] A. Hutt, A. Longtin, L. Schimansky–Geier, *Additive global noise delays Turing bifurcations*, Phys. Rev. Lett., **98,** (2007) 230601–230605.

[15] N. Iqbal, R. Wu, B. Liu, *Pattern formation by super–diffusion in FitzHugh–Nagumo model*, Appl. Math. Comput, **313,** (2017) 245–258.

[16] S. Javeed, A. Ahmed, M. S. Khan, M. A. Javed, *Stability Analysis and Solutions of Dynamical Models for Dengue*, Punjab Uni. J. Math. **50,** (2018), 45–67.

[17] J. S. McGough, D. Kay, K. Burrage, *Pattern formation in the Gray–Scott model*, Nonlinear Analysis: RWA., **5,** (2004) 105–121.

[18] R. Jiwari, S. Singh, A.Kumar, *Numerical simulation to capture the pattern formation of coupled reaction–diffusion models*, Chaos, Solitons and Fractals, **103,** (2017) 422–439.

[19] G. Li, Q. Ouyang, V. Petrov, H.L. Swinney, *Transition from simple rotating chemical spirals to meandering and traveling spirals*, Phys. Rev. Lett., **77,** (1996) 2105–2113.

[20] B. Liu, R. Wu, N. Iqbal, L. Chen, *Turing patterns in the Lengyel–Epstein system with superdiffusion*, Int. J. Bifurcat. Chaos, **27,** (2017) 1730026.
[21] P.K. Maini, K.J. Painter, H.N.P. Chau, *Spatial pattern formation in chemical and biological systems*, J. Chem. Soc. Faraday Trans., **93,** (1997) 3601–3610.
[22] H. Meinhardt, *Models of biological pattern formation*, Academic Press, New york, (1982).
[23] J. D. Murray, *Mathematical Biology*, Springer-Verlag, Berlin, 1993.
[24] S.V. Petrovskii, H. Malchow, *A minimal model of pattern formation in a prey–predator system*, Math. Comput. Model., **29,** (1999) 49–63.
[25] M. Pascual, *Diffusion–induced chaos in a spatial predator–prey system*, Proc. R. Soc. Lond. B: Biol. Sci., **251,** (1993) 1–7.
[26] F. de Pasquale, B. Spagnolo, *Stochastic Model of Population Dynamics, in Chaos and Noise in Biology and Medicine*, eds. M. Barbi and S. Chillemi World Scientific Biophysics, **7,** (1998) 305–314.
[27] J.A. Sherratt, *Periodic travelling waves in cyclic predator–prey systems*, Ecol. Lett., **4,** (2001) 30–37.
[28] J. Shukla, S. Verma, *Effects of convective and dispersive interactions on the stability of 2 species*, Bull. Math. Biol., **43,** (1981) 593–610.
[29] Y. Song, X. Zou, *Spatiotemporal dynamics in a diffusive ratio–dependent predator–prey model near a Hopf–Turing bifurcation point*, Comput. Math. Appl. **67**, (2014) 1978–1997.
[30] Y. Song, X. Zou, *Bifurcation analysis of a diffusive ratio-dependent predator–prey model*, Nonlinear Dynam., **78,** (2014), 49–70.
[31] B. Spagnolo, D. Valenti, A. Fiasconaro, *Noise in ecosystems: A short review*, Math. Biosci. Eng., **1,** (2004) 185–211.
[32] B. Spagnolo, A. Fiasconaro, D. Valenti, *Noise induced phenomena in Lotka–Volterra systems*, Fluct. Noise Lett., **3,** (2003) L177–L185 .
[33] C. Tian, L. Zhang, *Delay–driven irregular spatiotemporal patterns in a plankton system*, Phys. Rev. E, **88,** (2013) 012713–012719.
[34] C. Tian, L. Zhang, *Traveling wave governs the stability of spatial pattern in a model of allopathic competition interactions*, Chaos, **22,** (2012) 043136–043144.
[35] C. Tian, L. Lin, L. Zhang, *Additive noise driven phase transitions in a predator–prey system*, Appl. Math. Model., **46,** (2017) 423–432.
[36] A. M. Turing, *The chemical basis of morphogenesis*, Phil. Trans. R. Soc. Lond. B, **237,** (1952) 37–72.
[37] D. Valenti, A. Fiasconaro, B. Spagnolo, *Stochastic resonance and noise delayed extinction in a model of two competing species*, Phys. A, **331,** (2004) 477–486.
[38] D. Valenti, L. Schimansky–Geier, X. Sailer, B. Spagnolo, *Moment equations for a spatially extended system of two competing species*, Europ. Phys. J. B–Condens. Matter Complex Syst., **50,** (2006) 199–203.
[39] D. Valenti, G. Denaro, A.L. Cognata, B. Spagnolo, A. Bonanno, G. Basilone, S. Mazzola, S. Zgozi, S. Aronica, *Picophytoplankton dynamics in noisy marine environment*, Acta Phys. Polonica-Ser. B Elem. Part. Phys., **43,** (2012) 1227.
[40] A. R. Vieira, N. Crokidakis, *Phase transitions in the majority–vote model with two types of noises*, Physica A: Stat. Mech. and its App., **450,** (2016) 30–36.
[41] A. R. Vieira, N. Crokidakis, *Noise–induced absorbing phase transition in a model of opinion formation*, Physics Letters A, **380,** (2016) 2632–2636.
[42] W. Wang, Y. Lin, F. Yang, L. Zhang, Y. Tan, *Numerical study of pattern formation in an extended Gray–Scott model*, Commun. in Nonlinear Sci. and Num. Sim., **16,** (2011) 2016–2026.
[43] W. Wang, Q. Liu, Z. Jin, *Spatiotemporal complexity of a ratio–dependent predator–prey system*, Phys. Rev. E, **75,** (2007) 051913–051922.
[44] Z. Xu, Y. Song, *Bifurcation analysis of a diffusive predator–prey system with a herd behavior and quadratic mortality*, Math. Meth. Appl. Sci. (2014). http://dx.doi.org/10.1002/mma.3275.
[45] A. Yokuş, C*omparison of Caputo and conformable derivatives for time-fractional Korteweg-de Vries equation via the finite difference method.* International Journal of Modern Physics B, **32,** (2018) 1850365.
[46] A. Yokuş, *Numerical solution for space and time fractional order Burger type equation*, Alexandria Engineering Journal, 2017.
[47] S. Yuan, C. Xu, T. Zhang, *Spatial dynamics in a predator–prey model with herd behavior*, Chaos **23,** (2013), 0331023.

[48] X. Zhang, G. Sun, Z. Jin, *Spatial dynamics in a predator–prey model with Beddington–Deangelis functional response*, Phys. Rev. E, **85,** (2012) 021924–021938.

[49] Q. Zheng, J. Shen, *Pattern formation in the FitzHugh–Nagumo model*, Comp. and Math. with App., **70,** (2015) 1082–1097.

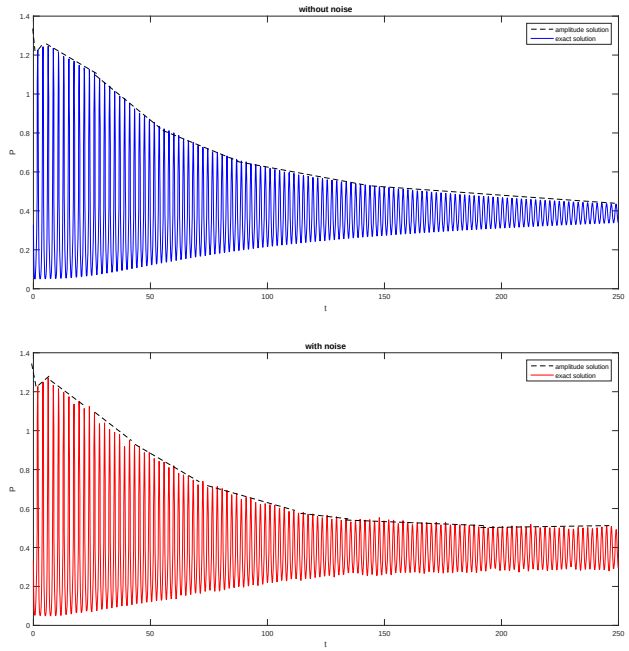

FIGURE 1. Comparability of prey P density for system (2.4) among deterministic system (up panel) and noise system (down panel). (Noise $\varphi = 0.01$, with parameters $r = 50, b = 0.572$.)

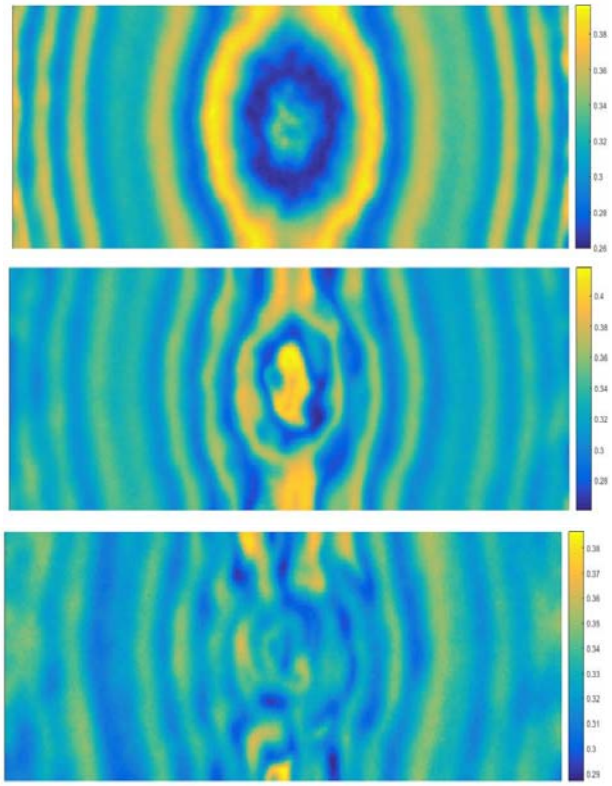

FIGURE 2. Spatial dispersion of P (prey) for (a) $t = 250$, (b) $t = 500$, (c) $t = 1000$, (d) $t = 2000$ having initial condition (4.19) for the system (2.4) with parameters $r = 50, b = 0.572, \varphi = 0.01$.

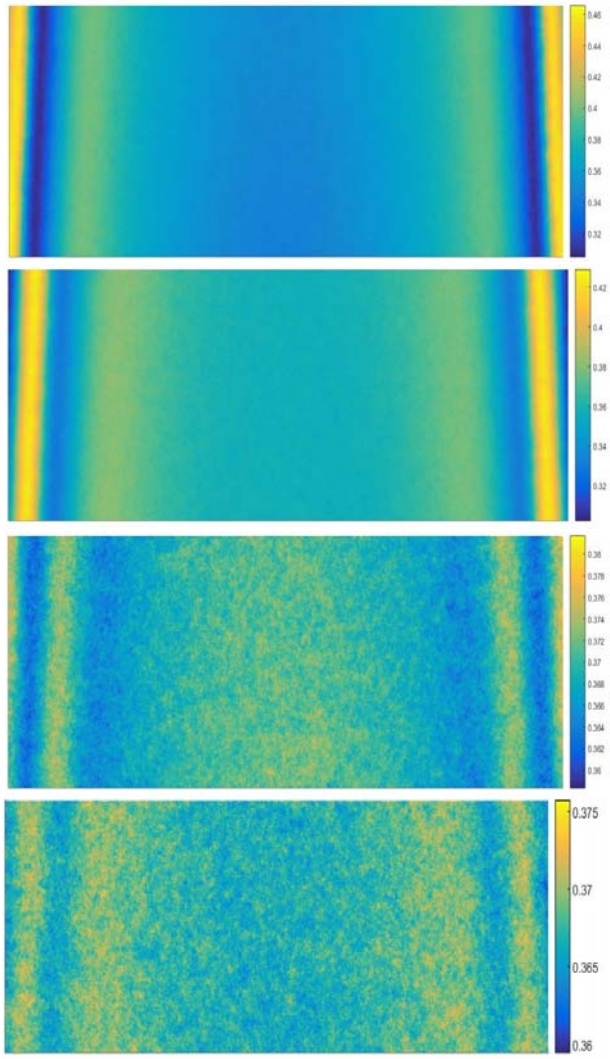

FIGURE 3. Spatial dispersion of P prey for (a) $t = 50$, (b) $t = 100$, (c) $t = 200$, (d) $t = 250$ having initial condition (4.19) for the system (2.4) with parameters $\alpha = 0.1, r = 50, b = 0.572, \varphi = 0.01$.

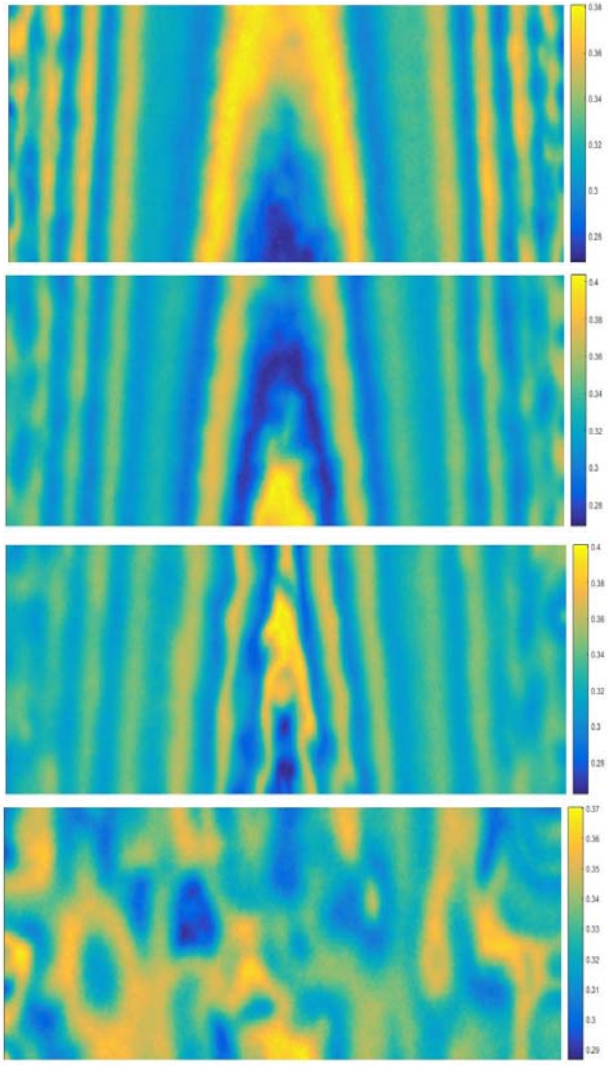

FIGURE 4. Spatial dispersion of P prey for (a) $t = 250$, (b) $t = 500$, (c) $t = 1000$, (d) $t = 2000$ having initial condition (4.20) for the system (2.4) with parameters $r = 50, b = 0.572, \varphi = 0.01$.

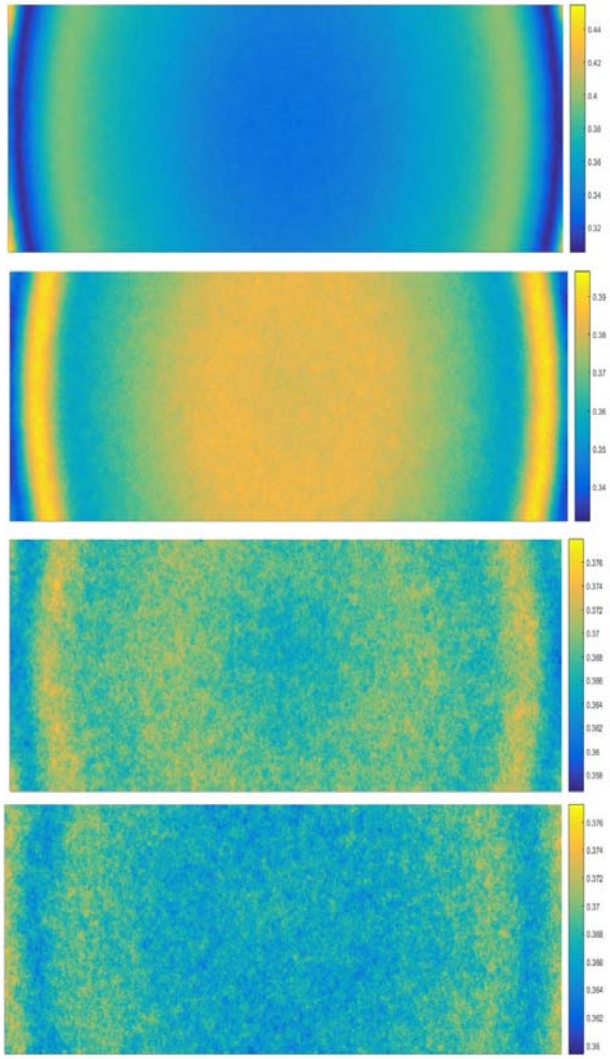

FIGURE 5. Spatial distribution of prey for (a) $t = 50$, (b) $t = 100$, (c) $t = 200$, (d) $t = 250$ with initial condition (4.20) for the system (2.4) with parameters $\alpha = 0.1, r = 50, b = 0.572, \varphi = 0.01$.

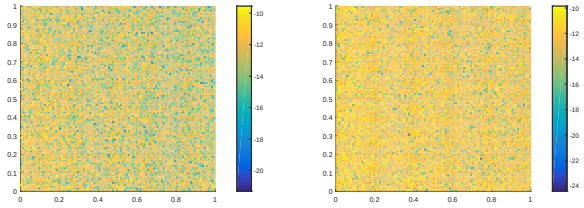

FIGURE 6. Images of 2-dimensional power spectra for P (prey) at $t = 2000$ with initial conditions (4.19) (left) and (4.20) (right).

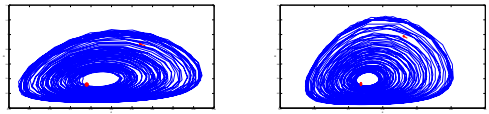

FIGURE 7. The System (2.4) phase plane at spatial location $(450, 150)$ in the filled domain by spatial–temporal irregular oscillation for initial conditions (4.19) (left) and (4.20) (right). The dot shows the initial point while the pointer indicates the trajectory direction.